International Journal on Magnetic Particle Imaging
Vol 8, No 1, Suppl 1, Article ID 2203068, 3 Pages

Proceedings Article

Increasing the efficiency of open-sided field free line scanning MPI system using silicon-steel core

Damla Alptekin Soydan*· Sefa Karaca · Can Barış Top

ASELSAN Research Center, Aselsan A.Ş., Ankara, Turkey
*Corresponding author, email: dasoydan@aselsan.com.tr

Abstract
Currently available preclinical magnetic particle imaging (MPI) systems can provide mm/sub mm -scale resolution for bore diameter of a few centimeters. A human-scale system that preserves mm-scale resolution requires large coil sizes and a high amount of current and power. Since the resolution in MPI mainly depends on the magnetic field gradient of the selection field coils, core loading may help to obtain a sufficient resolution with a feasible coil size and power consumption. Here, we present an open-sided small-size MPI system in which the outer selection field coils are loaded with a planar magnetic core. We investigated the effect of core loading on the magnetic field efficiencies and the impedances of the coils. For the measurements, three different types of silicon-steels with varying thicknesses are used as core material. Conducted simulation and experimental studies showed that gradient efficiency of the inner and outer coils can be increased by approximately 1.25 and 2 times, respectively.

I. Introduction

Magnetic Particle Imaging (MPI) is a safe imaging modality with a high sensitivity and spatiotemporal resolution, which make it suitable for different applications such as angiography, cell tracking, cancer, and inflammation imaging [1]. The feasibility of the MPI method has been shown by in-vitro and in-vivo studies, in which most of the utilized systems are small-sized preclinical systems with a limited bore diameter between 3 cm and 12 cm [2]. One of the difficulties in transition to a human-sized clinical MPI system is maintaining mm-scale resolution with large bore size. Since the image resolution mainly depends on the magnetic field gradient, selection field (SF) coils should provide sufficient gradient. Core-loaded SF coils generate higher magnetic field strength and lighten the size and power requirements. Therefore, they were preferred for both imaging [2, 3] and magnetic actuation [4–6] applications.

In [7], an open-sided field free line (FFL) based MPI system was proposed. Electronic scanning of the FFL was achieved using bi-planar coil configuration in both x- and y- directions. In the prototype system using this configuration, the outer coil group required approximately 10 times more power than the inner coil group to maintain the same magnetic field gradient level [8]. To decrease the total current and power requirements, outer coil group was loaded with a steel core in a simulated human-scale system [7]. The results have shown that both coil size and power can be decreased with magnetic core loading.

In this study, we designed a small-scale open-sided MPI system with 20 mm diameter circular field of view (FOV). The effect of steel loading on the efficiency of selection and drive coils in the system was analyzed experimentally for three different types of silicon-steel plates. We present both simulation and measurement results of the designed system.

10.18416/ijmpi.2022.2203068

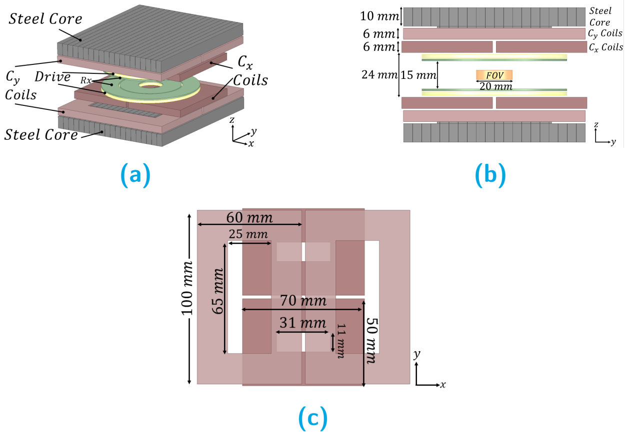

Figure 1: **(a)** Simulation model of the small-size magnetic core loaded MPI system. The coil dimensions are shown in **(b)** side view of the MPI system and **(c)** top view of the SF coils

Table 1: Coil properties for the core-loaded MPI system

Coil Type	Dimensions $x \times y$ (mm)	Height (mm)	Number of Turns
Cx	Inner 31×11 Outer 70×50	6	30
Cy	Inner 25×65 Outer 60×100	6	30
Drive	Inner Radius 10 Outer Radius 80	2	30

II. Material and methods

The small-size magnetic core loaded FFL scanning MPI system with 15 mm aperture height and 20 mm diameter FOV was designed using open-sided coil configuration (see Figure 1) [7], [8]. SF coils that generate FFL along the x-axis and y-axis are named as C_x coils and C_y coils, respectively. With this configuration, the FFL can be rotated to any direction on the xy-plane, and translated electronically in the field of view. Furthermore, the orthogonality between the magnetic field and its gradient enables tomographic imaging with single-axis drive and receive coils. For the detailed explanation of the coil arrangement, and FFL rotation and translation, interested readers can refer to [7], [8].

In the proposed MPI system, outer coil group (C_y coils in Figure 1) were loaded with planar silicon-steel laminations to increase the magnetic flux density and provide higher gradient field strength. The magnetic core was designed as thin steel sheets stacked in layers to prevent Eddy current losses [9]. For the simulations, each layer of the core was modeled with a height of 10 mm and thickness of 4.9 mm, assuming 0.1 mm thick coating layer between the plates. Steel was selected as *Steel-1008*, which is readily available in the material library of the simulator (Ansys Electromagnetics Suite, Ansys Inc., USA). The MPI system was designed to generate 0.5 T/m SF gradient, and 5 mT-peak drive field. The drive coil was designed in Helmholtz configuration. Coil parameters (size and number of turns) are given in Table 1.

For the experimental studies, silicon-steels (Si-Fe alloy) were preferred since the silicon addition improves the magnetic softness and decreases the Eddy currents by increasing the resistivity of the iron [9]. Loading with three different type of silicon-steel plates, with thicknesses of 0.23 mm, 0.35 mm, 0.65 mm were compared for the prototype system. The 0.23 mm thick silicon-steel is grain-oriented (i.e., magnetic permeability is direction-dependent), whereas 0.35 mm and 0.65 mm thick silicon-steels are non-grain-oriented. The core materials were procured from a local producer (Somal Steel, Turkey) as plates. The plates were cut and stacked in layers. The photographs of the stacked magnetic core and the produced prototype system are shown in Figure 2. Note that the thickness of the steel plates in the simulations were larger than the prototype system to decrease the number of mesh elements for computationally-efficient simulations. The housing of the coils was produced using a 3D printer. The selection (C_x and C_y) and the drive field coils were wounded using 200-strand×71 μm Litz wire (Rupalit V155, Pack Gmbh & Co., Germany).

Both magnetic field gradient and impedance values were measured for SF and drive coils in the system. For the magnetic field measurements, DC voltage generated using the waveform generator (33512B, Keysight Technologies, USA) was amplified using a AE Techron 7224 (AE Techron Inc, USA) amplifier. The current flowing through the coils was monitored using a 1146B current probe (Keysight Technologies, USA). The magnetic field was measured using a Lakeshore F71 Multiaxis Teslameter and a single axis Hall effect probe (Lake Shore Cryotronics Inc., OH, USA). For the SF coils, magnetic fields were measured at discrete positions along a line which is orthogonal to the FFL. Impedance measurements for the selection and drive coils were conducted at a frequency of 20 Hz and 25 kHz, respectively. The impedance of the upper and lower SF coils was measured separately, and results are given for lower coils only. The resistance and inductance of the coils were measured using E4980AL LCR meter (Keysight Technologies, USA).

III. Results

Simulation results are summarized in Table 2. The measured magnetic field efficiency and impedance results are summarized in Table 3 and Table 4, respectively. The magnetic field efficiencies inside the FOV, and the inductance values of the selection and drive coils were measured in the presence and absence of the magnetic core.

10.18416/ijmpi.2022.2203068

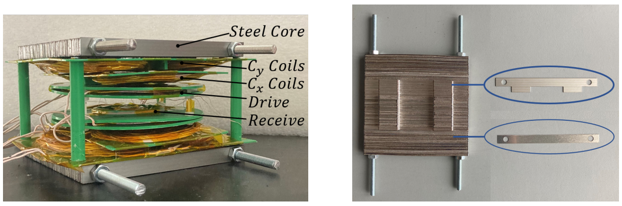

(a) (b)

Figure 2: **(a)** Thin laminated steel sheets were stacked in layers. **(b)** Silicon-steel core loaded open-sided MPI prototype

SF gradient efficiency and drive field efficiency were defined in terms of mT/m/A and mT/A, respectively.

Table 2: Simulation results for the Steel-1008-loaded MPI system (*For drive coils, the efficiency is defined in terms of mT/A)

Coil Type	Magnetic Field Eff. mT/m/A or mT/A*		Inductance (μH)	
	No Steel	*Steel 1008*	*No Steel*	*Steel 1008*
Cx	47	64	78	106
Cy	30	76	164	386
Drive*	1.0	1.4	100	130

Table 3: Magnetic field efficiency measurement results for silicon-steel loaded MPI system (*For drive coils, the efficiency is defined in terms of mT/A)

Coil Type	Magnetic Field Eff. mT/m/A or mT/A*			
	No Steel	*Steel 0.23 mm*	*Steel 0.35 mm*	*Steel 0.65 mm*
Cx	44	53	50	55
Cy	30	61	60	63
Drive*	0.85	1.2	1.1	1.1

Table 4: Impedance measurement results for silicon-steel loaded MPI system

Coil Type	Inductance (μH) / Resistance ($m\Omega$)			
	No Steel	*Steel 0.23 mm*	*Steel 0.35 mm*	*Steel 0.65 mm*
Cx	73 / 284	84 / 288	82 / 289	85 / 290
Cy	151 / 390	296 / 392	298 /394	299 / 392
Drive	97 / 412	112 / 636	113 / 751	111 / 971

IV. Conclusion

We have shown that magnetic core loading of the outer selection field coils improved the magnetic field strength of the both selection and drive coils for the open-sided scanner configuration. The efficiency of the C_x and C_y coils increased by approximately 25% and 100%, respectively. In the absence of the steel core, simulated and measured coil properties showed good agreement. On the other hand, measured coil efficiency was smaller compared to the simulated one, possibly due to the lower magnetic permeability of silicon-steels used in the measurements. It was observed that steel plates of different thicknesses had similar effects on the coil efficiency. We expected to get higher coil efficiency when the grain-oriented (0.23 mm thick) silicon-steel was used for core loading. However, there was no significant effect of using grain-oriented steel. This may be caused by the variation in the direction of the magnetic field created by the C_y coil group along the grain-oriented steel. The magnetic field was not aligned with the grain orientation along the C_y coil axes. In addition, the filling factor was lower for the grain oriented case, lowering the coil efficiency. Overall, the results imply that magnetic core loading can be used for mitigation of possible restrictions caused by power/current requirements of the outer coils in the open scanner configuration. Imaging performance of the designed system, and possible harmonic distortions due to the magnetic core should be studied further to optimize the image quality, while taking the power limitations into account.

Author's statement

Conflict of interest: Authors state no conflict of interest. Informed consent: Informed consent has been obtained from all individuals included in this study.

References

[1] B. Gleich and J. Weizenecker. Tomographic imaging using the non-linear response of magnetic particles. *Nature*, 435(7046), 2005.

[2] M. Graeser, F. Thieben, P. Szwargulski, F. Werner, N. Gdaniec, M. Boberg, F. Griese, M. Möddel, P. Ludewig, D. van de Ven, O. M. Weber, O. Woywode, B. Gleich, and T. Knopp. Human-sized magnetic particle imaging for brain applications. *Nature Comm.*, 2019.

[3] E. Yu. Hardware Innovations and Biomedical Applications of Magnetic Particle Imaging, PhD thesis. *UC Berkeley*, 2017.

[4] M. D. Tehrani, M. O. Kim, and J. Yoon. A Novel Electromagnetic Actuation System for Magnetic Nanoparticle Guidance in Blood Vessels. *IEEE Transactions on Magnetics*, 50(7), 2014.

[5] J. Rahmer, C. Stehning, and B. Gleich. Remote magnetic actuation using a clinical scale system. *Plos One*, 13(3), 2018.

[6] T.-A. Le, X. Zhang, A. K. Hoshiar, and J. Yoon. Real-Time Two-Dimensional Magnetic Particle Imaging for Electromagnetic Navigation in Targeted Drug Delivery. *Sensors*, 17, 2017.

[7] C. B. Top, S. Ilbey, and H. E. Güven. Electronically rotated and translated field-free line generation for open bore magnetic particle imaging. *Medical Physics*, 44(12), 2017.

[8] C. B. Top and A. Güngör. Tomographic field free line magnetic particle imaging with an open-sided scanner configuration. *IEEE Transactions on Medical Imaging*, 39(12), 2020.

[9] C. McLyman. Transformer and Inductor Design Handbook. *CRC Press*, 2017.

10.18416/ijmpi.2022.2203068